

## Ultrafast Intersystem Crossing in a Red Phosphorescent Iridium Complex

Gordon J. Hedley, Arvydas Ruseckas, and Ifor D. W. Samuel\*

*Organic Semiconductor Centre, SUPA, School of Physics and Astronomy, University of St Andrews, North Haugh, St Andrews, Fife, KY16 9SS, United Kingdom**Received: October 9, 2008*

Femtosecond photoluminescence (PL) and transient absorption (TA) studies have been carried out on the red phosphorescent metal complex tris(1-phenylisoquinoline)iridium(III) [Ir(piq)<sub>3</sub>] following excitation of the metal–ligand charge transfer singlet state. Rapid decay of the PL observed at 270 meV above the phosphorescence peak and TA dynamics are indicative of intersystem crossing, which occurs with a time constant of 70 fs. PL decays at 140 meV above the phosphorescence peak are biexponential with time constants of 95 fs and 3 ps, attributed to intramolecular vibrational redistribution (IVR) and vibrational cooling. The larger Ir(piq)<sub>3</sub> ligands facilitate faster dissipation of excess energy by IVR than the smaller Ir(ppy)<sub>3</sub> core.

## Introduction

Transition metal complexes show electronic and optical properties promising for applications in organic light emitting diodes (OLEDs)<sup>1</sup> and solar cells.<sup>2</sup> In contrast to fluorescent materials which have substantial losses due to injected charges combining to form nonemissive triplet states, transition metal complexes contain a heavy central metal atom that strongly mixes the emitting singlet and dark triplet states by spin–orbit coupling (SOC), thus enabling triplet emission with high efficiency. Strong SOC in iridium complexes<sup>3</sup> has enabled fabrication of OLEDs with internal efficiencies approaching 100%.<sup>4</sup> The lowest energy excited states are either metal–ligand charge transfer (MLCT)—where the highest occupied molecular orbital (HOMO) is a combination of both metal d orbitals and ligand  $\pi$  orbitals—or solely ligand centered, depending on the ligand chemical structure. Phosphorescence of both states is enhanced by SOC; however, the effect is stronger for MLCT emission due to the greater participation of the iridium electrons in the HOMO.<sup>5–8</sup>

Ultrafast spectroscopy provides valuable information on the nature of excited states and coupling between them. Previous ultrafast transient absorption (TA) studies showed contrasting results for the green phosphorescent Ir(ppy)<sub>3</sub> molecule. Tang et al. reported a finite risetime of the TA signal with time constants of 70 and 100 fs for different probe wavelengths.<sup>9</sup> In a later study of the same material an instantaneous rise of the TA signal was observed within 100 fs instrument response together with a constant TA on a longer time scale.<sup>10</sup> These results can be explained by the substantial spectral overlap of the absorption spectra from the singlet and triplet excited states, hence TA in the visible spectra region in Ir(ppy)<sub>3</sub> is not sensitive to intersystem crossing (ISC). Detection of fluorescence of singlet MLCT states has not yet been reported in iridium complexes.

In this letter we report short-lived photoluminescence (PL) from the singlet MLCT state and matching dynamics of TA in

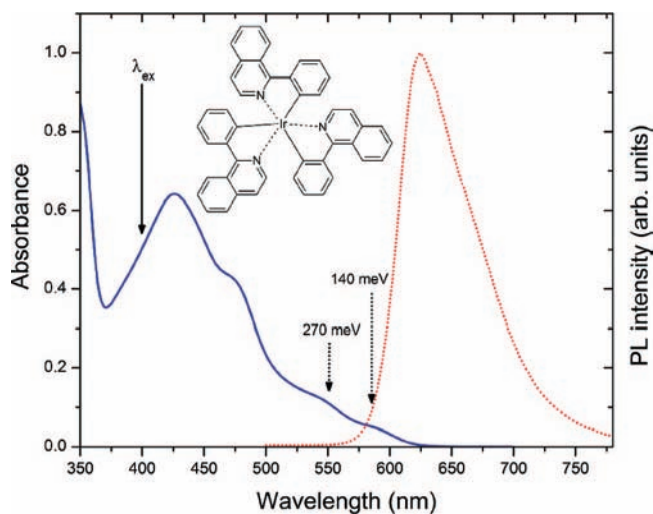


**Figure 1.** Absorption (solid line) and photoluminescence (dotted line) spectra of Ir(piq)<sub>3</sub> (structure shown in the inset). All studies have been performed with an excitation wavelength of 400 nm (solid arrow). The dotted arrows indicate detection wavelengths at different energies relative to the steady state phosphorescence peak.

a red-emitting iridium complex which allow us to determine the time constant for ISC as  $70 \pm 10$  fs. Phosphorescence from the hot triplet MLCT state is then observed and it decays faster when compared to a complex with a smaller ligand. This shows that vibrational relaxation occurs predominantly by intramolecular vibrational redistribution (IVR).

## Experimental Methods

The homoleptic tris(1-phenylisoquinoline)iridium(III)—denoted as Ir(piq)<sub>3</sub>, structure shown in the inset to Figure 1—provides deep red emission that satisfies the CIE color rendition requirements for full color displays, and gives OLEDs with a high external quantum efficiency of 10.3%.<sup>11</sup> Ir(piq)<sub>3</sub> powder was procured from American Dye Sources Inc., and was used without further purification. Solutions of the compound were

\* Corresponding author. Phone: +44 1334 463 114. Fax: +44 1334 463 104. E-mail: idws@st-andrews.ac.uk.

prepared by dissolving it in tetrahydrofuran (THF) (spectroscopic grade, Sigma Aldrich Co.) at a concentration of 1 mg in 1 mL. Ultrafast PL dynamics were measured with use of the femtosecond optical gating (FOG) technique. The excitation source was the frequency doubled output from a Ti:Sapphire oscillator with pulses of 100 fs (fwhm) at 80 MHz. The 400 nm excitation was focused on the sample and the residual 800 nm sent down a delay line path before acting as the gating pulse. Optical gating was achieved by sum-frequency mixing of the luminescence photons from the sample and the gating pulse in a BBO nonlinear crystal. Upconverted luminescence was spatially and spectrally filtered before being detected with a photomultiplier tube. The instrument response function (IRF) of the setup was recorded by upconverting 400 nm excitation pulses, and an IRF of 260 fs (fwhm) was found. Transient absorption (TA) studies were undertaken with an amplified Ti:Sapphire laser system, with a delayable 400 nm, 100 fs (fwhm), 2.5 kHz synchronously chopped pump and the tuneable output from a noncollinear optical parametric amplifier (500–1000 nm), 30–50 fs (fwhm) acting as the probe. Probe energies were kept constant at 3 nJ; a reference was recorded at 5 kHz and the signal at 2.5 kHz. The IRF of the TA setup was 150 fs (fwhm). A rotating sample cell (optical path length 0.5 mm) was used to minimize photodegradation for both FOG and TA measurements. The absence of photodegradation was confirmed by regular checks of the solution's absorption and PL spectra.

## Results

Steady state absorption and PL spectra for Ir(piq)<sub>3</sub> are shown in Figure 1, with the chemical structure of the molecule inset to the figure. The singlet and triplet MLCT absorption features have been previously assigned,<sup>11</sup> with the shoulder at 600 nm representing the <sup>3</sup>MLCT ← S<sub>0</sub> transition and having a significant admixture of singlet character, and the shoulder at 550 nm representing the <sup>1</sup>MLCT ← S<sub>0</sub> transition. Figure 2a shows the recorded luminescence dynamics at 550 nm (270 meV above the PL peak), a wavelength at which there is no steady state emission. The PL decays extremely quickly and can be fitted by convolving a decay time of 70 fs with the IRF. We note that Raman signals from the solvent were at much shorter wavelengths (<480 nm) and so would not affect the recorded dynamics. Figure 2b shows the PL dynamics from the hot <sup>3</sup>MLCT state detected at 140 meV above the steady state PL peak. The PL decay is faster in Ir(piq)<sub>3</sub> than in the smaller Ir(ppy)<sub>3</sub> at the same value of energy above its PL peak. The best fit to a two-exponential decay function gives time constants (and pre-exponential factors) of 95 fs (96%) and 3 ps (4%) for Ir(piq)<sub>3</sub>, whereas in Ir(ppy)<sub>3</sub> they are 150 fs (88%) and 3 ps (12%). Figure 3 shows transient absorption kinetics at probe wavelengths of 600 and 675 nm, where the signal at both wavelengths is positive, representing excited state absorption (ESA). When probing at 675 nm a partial decay is observed—the long-lived signal shows no decay on a picosecond time scale. Fitting to an exponential decay function gives a time constant of 74 ± 10 fs representing 33(±3)%—the rest of the amplitude consisting of an offset representing dynamics longer than 1 ns. A matching risetime of 70 ± 20 fs fits the kinetics when probing at 600 nm and constitutes 35(±15)% of the total amplitude (the rest being instrument limited).

## Discussion

As the shoulder at 550 nm in the absorption spectrum has been assigned to the <sup>1</sup>MLCT ← S<sub>0</sub> transition,<sup>11</sup> the rapid decay of the PL at this wavelength, as shown in Figure 2a, is attributed

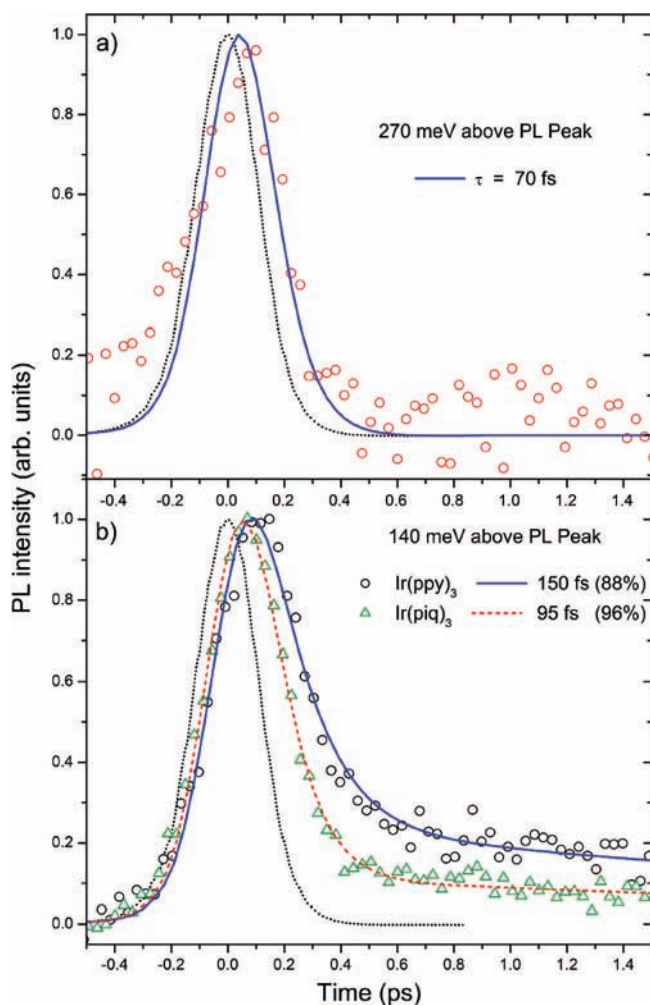


**Figure 2.** (a) Femtosecond luminescence of Ir(piq)<sub>3</sub> at 550 nm, on the <sup>1</sup>MLCT absorption shoulder. The dotted line is the IRF. The solid line is a fit to an exponential decay with a lifetime of 70 fs, which is assigned to a <sup>1</sup>MLCT emission. (b) Ultrafast luminescence dynamics for Ir(piq)<sub>3</sub> (open triangles) and Ir(ppy)<sub>3</sub> (open circles) at 140 meV above their respective phosphorescence peaks. Best-fits are indicated with solid lines for both decays, with time constants of 95 fs (96%) for Ir(piq)<sub>3</sub> and 150 fs (88%) for Ir(ppy)<sub>3</sub>, with the remainder of the decay accounted for by a 3 ps component for both compounds. The IRF is indicated as a dotted line. Ir(ppy)<sub>3</sub> data in this panel are from ref 18.

to the relaxation of the <sup>1</sup>MLCT state with a time constant of 70 fs. Transient absorption studies, shown in Figure 3, complement this conclusion, and indeed support that this 70 fs process is assigned to ISC. The ESA of complexes with MLCT excitation is dominated by  $\pi$ - $\pi^*$  absorption of the reduced ligand from 400 to 700 nm.<sup>12</sup> The highest occupied molecular orbital of iridium complexes is a mixture of the d orbitals of iridium and  $\pi$  orbitals of the ligand.<sup>5</sup> Upon photoexcitation there is a decrease of electron density in the  $\pi$  orbital of the ligand. In the inset to Figure 3 this is illustrated as a reduction in the density of the electrons with spin down orientation. As the  $\pi$ - $\pi^*$  absorption of the reduced ligand has to be a spin-allowed transition, a higher density of electrons with spin up orientation in the  $\pi$  orbital will give a stronger signal in the <sup>1</sup>MLCT than in the <sup>3</sup>MLCT state. This explains the 70 ± 10 fs decay in the transient absorption signal at longer wavelengths. Consequently the 70 ± 20 fs risetime observed at shorter wavelengths suggests stronger <sup>3</sup>MLCT absorption to higher energy  $\pi$ - $\pi^*$  excited states than <sup>1</sup>MLCT absorption. The combination of PL and TA dynamics provides the first direct observation of ISC in iridium

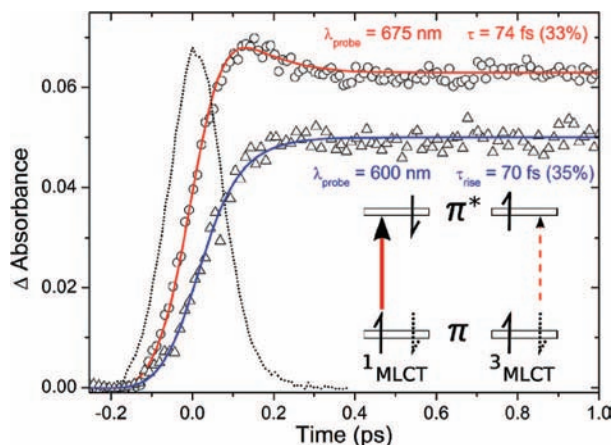


**Figure 3.** Ultrafast transient absorption kinetics ( $\lambda_{\text{pump}} = 400 \text{ nm}$ ) of  $\text{Ir}(\text{piq})_3$ . Solid lines show best-fits. Probing at 675 nm (upper trace) gives a best-fit decay of 74 fs representing 33% of the total decay amplitude—the other 67% being a greater than 1 ns offset. Probing at 600 nm (lower trace) gives a best-fit risetime of 70 fs representing 35% of the total formation—the other 65% being within the instrument limit. The IRF is indicated as a dotted line. The inset shows the schematic of the frontier ligand orbitals, showing the greater probability of  $\pi-\pi^*$  absorption in the  $^1\text{MLCT}$  state, as discussed in the text.

complexes to the best of our knowledge. Previous transient absorption studies have not provided conclusive evidence on the rate of this process.<sup>9,10</sup> Intersystem crossing on a similar time scale to that found here has been reported in ruthenium complexes,<sup>13–15</sup> iron complexes,<sup>16</sup> and rhenium complexes.<sup>17</sup> The red emitting material investigated in this work has more suitable ultrafast photophysical properties than those previously observed in iridium materials, allowing the singlet luminescence as well as transient absorption dynamics to be observed, enabling direct assignment of the ISC rate in  $\text{Ir}(\text{piq})_3$ .

The femtosecond and picosecond luminescence dynamics observed at 140 meV above the PL peak, Figure 2b, can be attributed to energy dissipation by intramolecular vibrational redistribution (IVR) and vibrational cooling, respectively.<sup>10,18</sup> The lifetime of the femtosecond component is shorter in  $\text{Ir}(\text{piq})_3$  compared to  $\text{Ir}(\text{ppy})_3$ , which indicates that the larger ligand enables faster energy dissipation by IVR. Similar behavior has been observed in  $\text{Ir}(\text{ppy})_3$ -cored dendrimers;<sup>18</sup> however, no rate increase was observed in that case. The enhancement of the IVR rate is higher in  $\text{Ir}(\text{piq})_3$  because here the chemical additions are more strongly connected to the ligand, as the extra phenyl in  $\text{Ir}(\text{piq})_3$  is fused onto the pyridine, rather than mediated through the single C–C bond, as in the dendrimers. This fusing ensures that energy flow can easily proceed in  $\text{Ir}(\text{piq})_3$ , without any barrier, and hence the increase in the rate of IVR is measurable and obvious.

The schematics of the ultrafast photophysical processes in  $\text{Ir}(\text{piq})_3$  are shown in Figure 4.

## Conclusions

To summarize, a short-lived emission from the singlet MLCT state with a 70 fs lifetime is observed in the red emitting phosphorescent metal complex  $\text{Ir}(\text{piq})_3$ . This time constant is consistent with dynamics observed in complementary transient absorption experiments, where a risetime at short probe

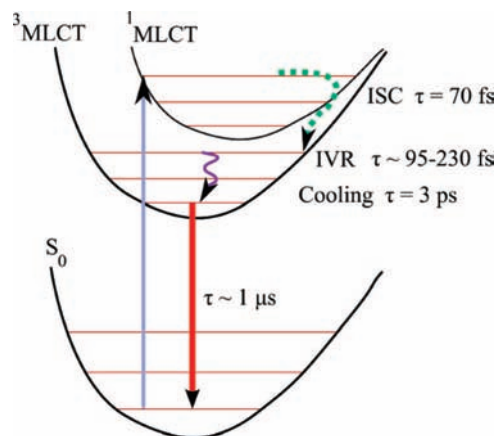


**Figure 4.** Schematic diagram outlining the ultrafast photophysical processes in  $\text{Ir}(\text{piq})_3$ . Energy spacings are not to scale.

wavelengths and decay at long probe wavelengths of 70 fs is recorded. Luminescence and transient absorption kinetics thus give strong evidence that the time constant of ISC in  $\text{Ir}(\text{piq})_3$  is  $70 \pm 10 \text{ fs}$ . At 140 meV above the phosphorescence steady state peak the femtosecond PL decay component is found to become measurably faster in  $\text{Ir}(\text{piq})_3$  compared to  $\text{Ir}(\text{ppy})_3$ , from 150 to 95 fs. This is indicative that the larger ligand of  $\text{Ir}(\text{piq})_3$ , which has a higher density of vibrational states, enables faster internal dissipation of excess energy by IVR.

**Acknowledgment.** The authors acknowledge EPSRC for financial support.

## References and Notes

- (1) Baldo, M. A.; O'Brien, D. F.; You, Y.; Shoustikov, A.; Sibley, S.; Thompson, M. E.; Forrest, S. R. *Nature* **1998**, *395*, 151.
- (2) Oregan, B.; Gratzel, M. *Nature* **1991**, *353*, 737.
- (3) King, K.; Spellane, P.; Watts, R. *J. Am. Chem. Soc.* **1985**, *107*, 1431.
- (4) Adachi, C.; Baldo, M. A.; Thompson, M. E.; Forrest, S. R. *J. Appl. Phys.* **2001**, *90*, 5048.
- (5) Hay, P. J. *J. Phys. Chem. A* **2002**, *106*, 1634.
- (6) Matsushita, T.; Asada, T.; Koseki, S. *J. Phys. Chem. C* **2007**, *111*, 6897.
- (7) Jansson, E.; Minaev, B.; Schrader, S.; Agren, H. *Chem. Phys.* **2007**, *333*, 157.
- (8) Nozaki, K. *J. Chin. Chem. Soc.* **2006**, *53*, 101.
- (9) Tang, K. C.; Liu, K. L.; Chen, I. C. *Chem. Phys. Lett.* **2004**, *386*, 437.
- (10) Hedley, G. J.; Ruseckas, A.; Samuel, I. D. W. *Chem. Phys. Lett.* **2008**, *450*, 292.
- (11) Tsuboyama, A.; Iwawaki, H.; Furugori, M.; Mukaide, T.; Kamatani, J.; Igawa, S.; Moriyama, T.; Miura, S.; Takiguchi, T.; Okada, S.; Hoshino, M.; Ueno, K. *J. Am. Chem. Soc.* **2003**, *125*, 12971.
- (12) McCusker, J. K. *Acc. Chem. Res.* **2003**, *36*, 876.
- (13) Benko, G.; Kallioinen, J.; Korppi-Tommola, J. E. I.; Yartsev, A. P.; Sundstrom, V. *J. Am. Chem. Soc.* **2002**, *124*, 489.
- (14) Bhasikuttan, A. C.; Suzuki, M.; Nakashima, S.; Okada, T. *J. Am. Chem. Soc.* **2002**, *124*, 8398.
- (15) Cannizzo, A.; van Mourik, F.; Gawelda, W.; Zgrablic, G.; Bressler, C.; Chergui, M. *Angew. Chem., Int. Ed.* **2006**, *45*, 3174.
- (16) Gawelda, W.; Cannizzo, A.; Pham, V. T.; vanMourik, F.; Bressler, C.; Chergui, M. *J. Am. Chem. Soc.* **2007**, *129*, 8199.
- (17) Cannizzo, A.; Blanco-Rodriguez, A. M.; El Nahhas, A.; Sebera, J.; Zalis, S.; Vlcek, J. A.; Chergui, M. *J. Am. Chem. Soc.* **2008**, *130*, 8967.
- (18) Hedley, G. J.; Ruseckas, A.; Liu, Z. H.; Lo, S. C.; Burn, P. L.; Samuel, I. D. W. *J. Am. Chem. Soc.* **2008**, *130*, 11842.